SUPPORTING INFORMATION

Metal-based flocculation to harvest microalgae: a look beyond separation efficiency

S. Rossi[1], S. Visigalli[1], F. Castillo Cascino[2], M. Mantovani[3], V. Mezzanotte[3], K. Parati[2], R. Canziani[1], A. Turolla[1], E. Ficara[1*]

[1] Politecnico di Milano, Department of Civil and Environmental Engineering (DICA), P.zza L. da Vinci, 3, 20133 Milan, Italy

[2] Istituto Sperimentale Italiano Lazzaro Spallanzani, Località La Quercia, 26027 Rivolta d'Adda, Italy

[3] Università degli Studi di Milano-Bicocca, Department of Earth and Environmental Sciences (DISAT), P.zza della Scienza 1, 20126 Milan, Italy

[*] Corresponding author (elena.ficara@polimi.it, +39 02 2399 6240)

Including: Table of contents, 6 Figures, 4 Tables, 12 Equations, and 7 References

16 **TABLE OF CONTENTS**

SI.1. EVOLUTION OF ENVIRONMENTAL CONDITIONS IN THE OUTDOOR SYSTEM

In this section, the evolution of light intensity for the outdoor cultivation system is reported. The light intensity is referred to the four days preceding the execution of the photo-respirometric test, as it was shown that this time interval is best correlated with the biomass activities in outdoor systems[1] (**Figure SI.1**).

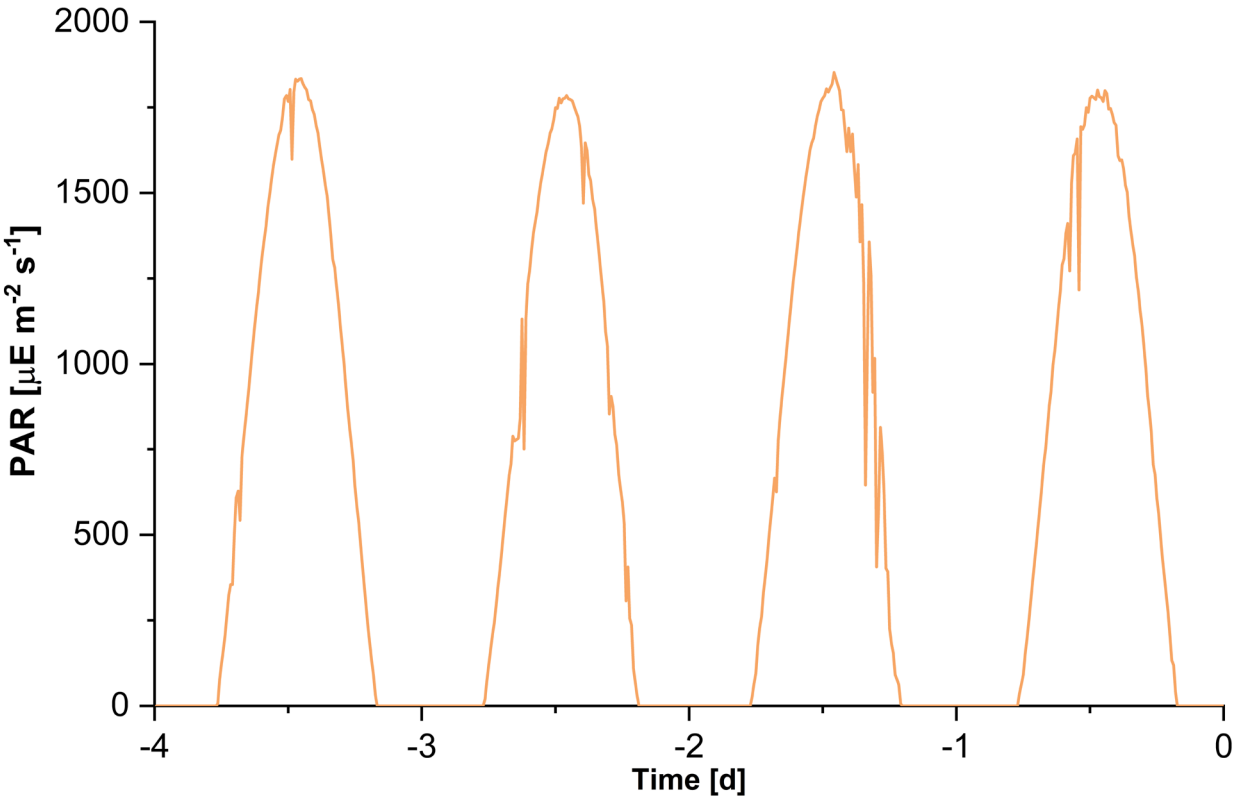

Figure SI.1. Variation of light intensity recorded for the microalgae-bacteria system growing in outdoor conditions (MBO), during the four days preceding the execution of the photo-respirometric test.

SI.2. COMPOSITION OF THE NUTRIENT-FREE MEDIUM USED TO DILUTE ALGAL-BACTERIAL SUSPENSIONS AND OF THE MODIFIED BOLD'S BASAL MEDIUM

Biomass samples were diluted using a synthetic nutrient-free medium, similar to the one fed to the PBR. MA samples were grown using a medium with constant characteristics over time, therefore they could be simply diluted in the cultivation BBM. For microalgae-bacteria samples MBI and MBO, the characteristics of LFAD varied over time, therefore a synthetic medium was used to reproduce the LFAD in terms of average ionic and micronutrients composition. The composition of the synthetic medium is reported in **Table SI.1**. The medium was used with no further modifications to dilute MBO samples. For MBI samples, a mixture of the same medium (10%) and nutrient-free MBBM (90%) was used. The composition of the MBBM is given in **Table SI.2**.

Table SI.1. Composition of the nutrient-free mineral medium used to dilute algal-bacterial suspensions in this study. Values are reported as mean ± standard deviation (n = 15).

ELEMENT	SYMBOL	UNIT	VALUE	SALT USED
Potassium	K	[mg L^{-1}]	22.6 ± 4.6	KCl
Magnesium	Mg	[mg L^{-1}]	19.6 ± 1.8	$MgSO_4 \cdot 7H_2O$
Calcium	Ca	[mg L^{-1}]	121 ± 29	$CaCl_2 \cdot 2H_2O$
Iron	Fe	[mg L^{-1}]	0.08 ± 0.07	$FeSO_4 \cdot 7H_2O$
Sodium	Na	[mg L^{-1}]	58.2 ± 7.9	NaCl
Zinc	Zn	[mg L^{-1}]	0.22 ± 0.61	$ZnSO_4 \cdot 7H_2O$
Manganese	Mn	[µg L^{-1}]	21.5 ± 11.9	$MnCl_2 \cdot 4H_2O$
Aluminium	Al	[µg L^{-1}]	0.06 ± 0.2	$Al_2(SO_4)_3$
Nickel	Ni	[µg L^{-1}]	22.9 ± 12.1	$NiCl_2 \cdot 6H_2O$
Copper	Cu	[µg L^{-1}]	22.3 ± 22.5	$CuSO_4 \cdot 5H_2O$

52 **Table SI.2.** Composition of the modified Bold's Basal Medium (MBBM).

PARAMETER	VALUE	UNIT
NH_4Cl	157.4	mg L^{-1}
$MgSO_4*7H_2O$	75.0	mg L^{-1}
NaCl	25.0	mg L^{-1}
K_2HPO_4	75.0	mg L^{-1}
KH_2PO_4	175.0	mg L^{-1}
$CaCl_2*2H_2O$	25.0	mg L^{-1}
$ZnSO_4*7H_2O$	8.82	mg L^{-1}
$MnCl_2*4H_2O$	1.44	mg L^{-1}
MoO_3	0.71	mg L^{-1}
$CuSO_4*5H_2O$	1.57	mg L^{-1}
$Co(NO_3)2*6H_2O$	0.49	mg L^{-1}
H_3BO_3	11.4	mg L^{-1}
EDTA	50.0	mg L^{-1}
KOH	31.0	mg L^{-1}
$FeSO_4*7H_2O$	4.98	mg L^{-1}
H_2SO_4	1.0	mL L^{-1}
$NaHCO_3$	175.0	mg L^{-1}

53

SI.3. DESCRIPTION OF PHOTO-RESPIROMETRY PROTOCOLS

Two standardized protocols adopted in this work were adapted from previous experiments: the DRIP and the SCIP. The DRIP was adopted to model dose-response curves for the biomass exposed to metallic flocculants ($FeCl_3$ and $Al_2(SO_4)_3$) and to a non-toxic flocculant (cationic starch). The DRIP was not modified from its original conception[3], and it was constituted by the repetition of L/D phases in a control reactor and in an inhibited reactor. In the inhibited reactor, the flocculant concentration is also increased at each L/D cycle. The SCIP was used to assess the value of the inhibition function at certain concentrations of the same flocculants tested with the DRIP, and to assess long-term effects after 24 h of exposure to metallic flocculants. The SCIP was adapted to describe inhibition, starting from a previously proposed photo-respirometric protocol designed to assess the effect of environmental conditions on the algal biomass[2]. The original protocol considered several repetitions of 3 L/D phases, under a wide range of conditions for each environmental parameter considered. In this case, the protocol was shortened to include only one L/D repetition, performed in the control and inhibited conditions. The succession of phases in the control and in the inhibited photo-respirometer are reported in **Table SI.3** for the DRIP and SCIP. Relevant simulated outputs for the DRIP and SCIP are also provided in **Figure SI.2** for an easier interpretation.

Table SI.3. Description of the photo-respirometric protocols used in this study.

PHASE	DURATION	SCIP		DRIP	
L/D	min	Control	Inhibited	Control	Inhibited
Pre-treatments	30-45	D-CR, LA			
L_1	5	NA*, ATU*	NA*, ATU*, FA	NA*, ATU*	NA*, ATU*, FA1
D_1	10	-	-	-	-
L_2	5	-	-	-	F2
D_2	10	-	-	-	-
L_3	5	-	-	-	F3
D_3	10	-	-	-	-
L_4	5	n.i.	n.i.	n.i.	F4
D_4	10	n.i.	n.i.	n.i.	-

Notes: (*) Only for MBI and MBO. Abbreviations: D: dilution, CR: centrifugation and resuspension, LA: light acclimation, NA: nutrient addition, ATU: allyl-thiourea addition, FA: flocculant addition, n.i. not included.

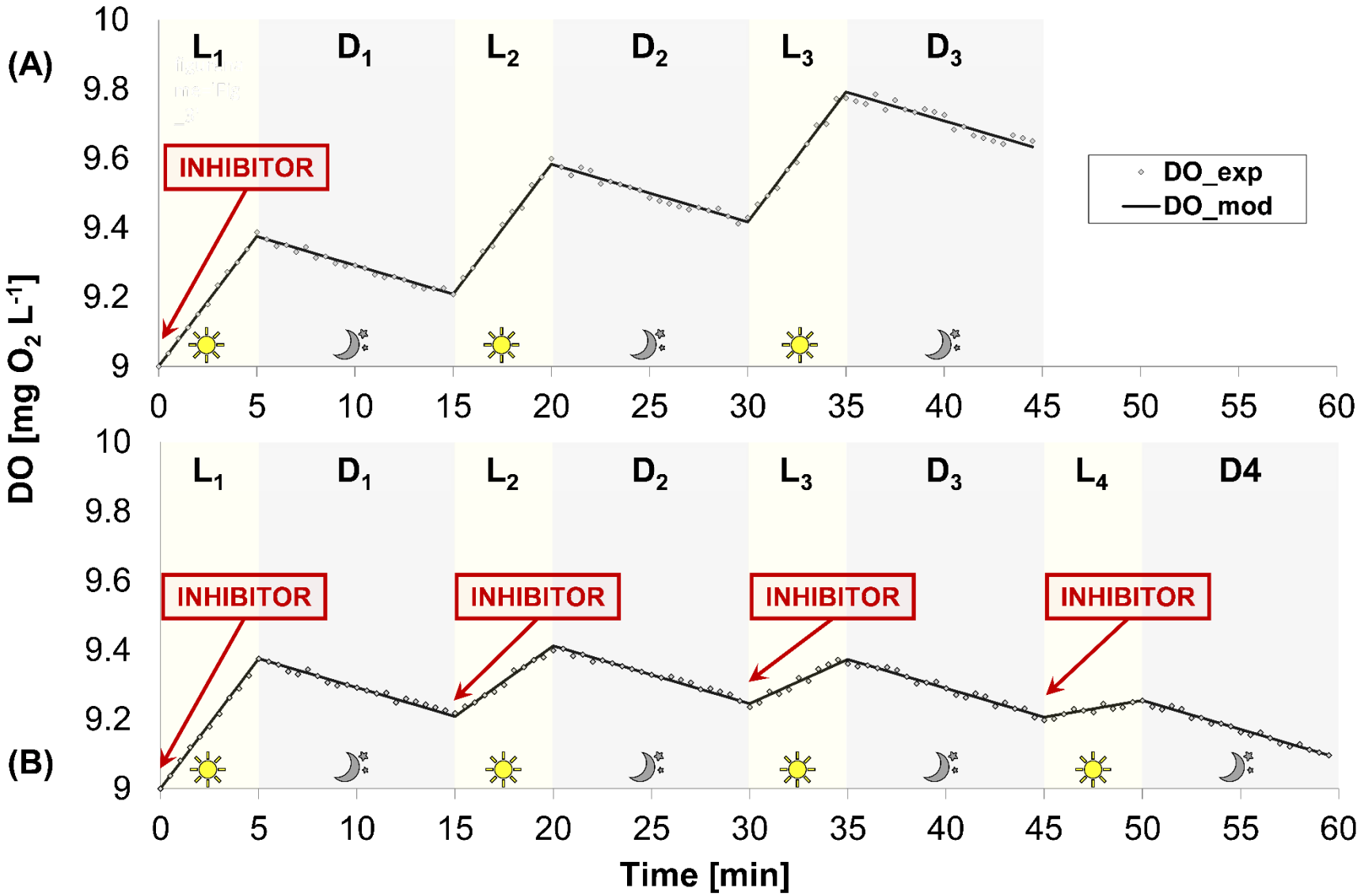

Figure SI.2. Simulated output of photo-respirometric tests and phases constituting the photo-respirometric inhibition protocols. Repetition of L/D phases in the control reactor of the SCIP and DRIP (A), repetition of L/D phases in the inhibited reactor of the DRIP (B). In the inhibited reactor of the SCIP, the inhibitor is dosed before the first light phase L_1. Light phases are indicated in yellow, dark phases are indicated in light grey.

SI.4. CALCULATION OF OXYGEN MASS BALANCES, PHOTOSYNTHESIS INHIBITION AND GOODNESS OF FIT

DO mass balance and data processing

The DO mass balance of the respirometer is:

$$\begin{cases} \frac{d(DO)}{dt} = OPR_{NET,L_i} + OTR \quad (i=1,\ldots,N) \\ \frac{d(DO)}{dt} = OUR_{RESP,D_i} + OTR \quad (i=1,\ldots,N) \end{cases} \qquad \text{(Eq. SI.1)}$$

Where: t is the experimental time [h]; N is the number of L/D cycles in the photo-respirometric protocol (N = 3 in the control reactor, and N = 4 in the inhibited reactor).

The DO concentration at saturation in the liquid (DO_{SAT}, [mg O_2 L^{-1}]) is:

$$DO_{SAT} = pO_2 \cdot H_{O_2}(T_{REF,H}) \cdot \exp\left(\frac{-\Delta_{SOL}H}{R} \cdot \left(\frac{1}{T} - \frac{1}{T_{REF,H}}\right)\right) \qquad \text{(Eq. SI .2)}$$

Where pO_2 = 0.21 [Atm] is the partial oxygen pressure in atmospheric air; $H_{O2}(T_{REF,H})$ = 40.5 [mg O_2 L^{-1} Atm^{-1}] is the reference value for the solubility constant of Henry's law[5]; $T_{REF,H}$ = 298.15 [K] is the reference temperature for the solubility constant H_{O2}; $\Delta_{SOL}H/R$ = 1200 [K] is the tabulated ratio between the Henry's solubility constant and the universal gas constant[5].

The OTR can be calculated as:

$$OTR = \theta^{(T-T_{REF,kLa})} \cdot kLa(T_{REF,kLa}) \cdot (DO_{SAT} - DO) \qquad \text{(Eq. SI .3)}$$

Where θ = 1.024 [-] is the recommended k_La temperature correction factor[6]; $T_{REF,kLa}$ = 293.15 [K] is the reference temperature for k_La; $k_La(T_{REF,kLa})$ = 0.114 [h^{-1}] is the volumetric mass transfer coefficient in the photo-respirometer, evaluated at the reference temperature[6].

The specific OPR_{GROSS} ($sOPR_{GROSS}$, **Equation SI.4**) can be obtained as:

$$sOPR_{GROSS,i} = \frac{OPR_{GROSS,i}}{TSS} = \frac{(OPR_{NET,i} - OUR_{RESP,i})}{TSS} \quad (i=1,\ldots,N) \qquad \text{(Eq. SI .4)}$$

Modelling of photosynthesis inhibition

The equation describing the reduction of the biological activity (f_I [-]) is:

$$f_I = \frac{sOPR_{GROSS,I}}{sOPR_{GROSS,CTRL}} = \frac{1}{1+\frac{I}{IC_{50}}} \quad \text{(Eq. SI .5)}$$

Where: $sOPR_{GROSS,I}$ is the microalgal specific gross oxygen production rate in the inhibited reactor [mg O_2 g TSS^{-1} h^{-1}]; $sOPR_{GROSS,CTRL}$ is the microalgal specific gross oxygen production rate in the control reactor [mg O_2 g TSS^{-1} h^{-1}]; I is the inhibitor concentration [mg L^{-1}].

Fitting techniques and goodness of fit

The adjusted R-squared (R_{ADJ}^2), the Root Mean Squared Error (RMSE), the Theil's Inequality coefficient (TIC), and the Mean Absolute Relative Error (MARE) can be expressed as follows:

$$R_{ADJ}^2 = 1-(1-R^2)\cdot\left(\frac{n-1}{n-p}\right) \quad \text{(Eq. SI .6)}$$

$$RMSE = \sqrt{\frac{\sum_j \left(y_{MEAS,j}-y_{MOD,j}\right)^2}{n}} \quad (j=1,\ldots,n) \quad \text{(Eq. SI .7)}$$

$$TIC = \frac{\sqrt{\sum_j \left(y_{MOD,j}-y_{MEAS,j}\right)^2}}{\sqrt{\sum_j \left(y_{MOD,j}\right)^2}+\sqrt{\sum_j \left(y_{MEAS,j}\right)^2}} \quad (j=1,\ldots,n) \quad \text{(Eq. SI .8)}$$

$$MARE = \frac{1}{n}\cdot\sum_j \frac{\left|y_{MEAS,j}-y_{MOD,j}\right|}{\left(y_{MEAS,j}+\varphi\right)} \quad (j=1,\ldots,n) \quad \text{(Eq. SI .9)}$$

Where R^2 is the computed coefficient of correlation of the model [-]; n is the number of experimental points [-]; p is the number of parameters of the fitted model [-]; y_{MEAS} is the measured variable under assessment; y_{MOD} is the modelled variable under assessment; $\varphi = 10^{-2}$ [-] is a small factor to avoid the division by zero.

SI.5. DETERMINATION OF THE VOLUMETRIC MASS TRANSFER COEFFICIENT

The volumetric mass transfer coefficient (kLa) was determined according to ASCE guidelines[6]. The photo-respirometers were set up as during normal operations, but filled up with tap water. The water was then de-oxygenated using concentrated solutions of sodium sulphite (Na_2SO_3) and cobalt catalyst ($CoCl_2 \cdot 6H_2O$). The sodium sulphite was dosed according to the DO concentration (7.88 mg Na_2SO_3 mg DO^{-1}) and with a stochiometric excess of 200%. The cobalt catalyst was dosed at 0.5 mg Co L^{-1}. The resulting mass transfer coefficient was almost identical for the two reactors (relative error lower than 0.2 %), with kLa = 1.14 h^{-1}.

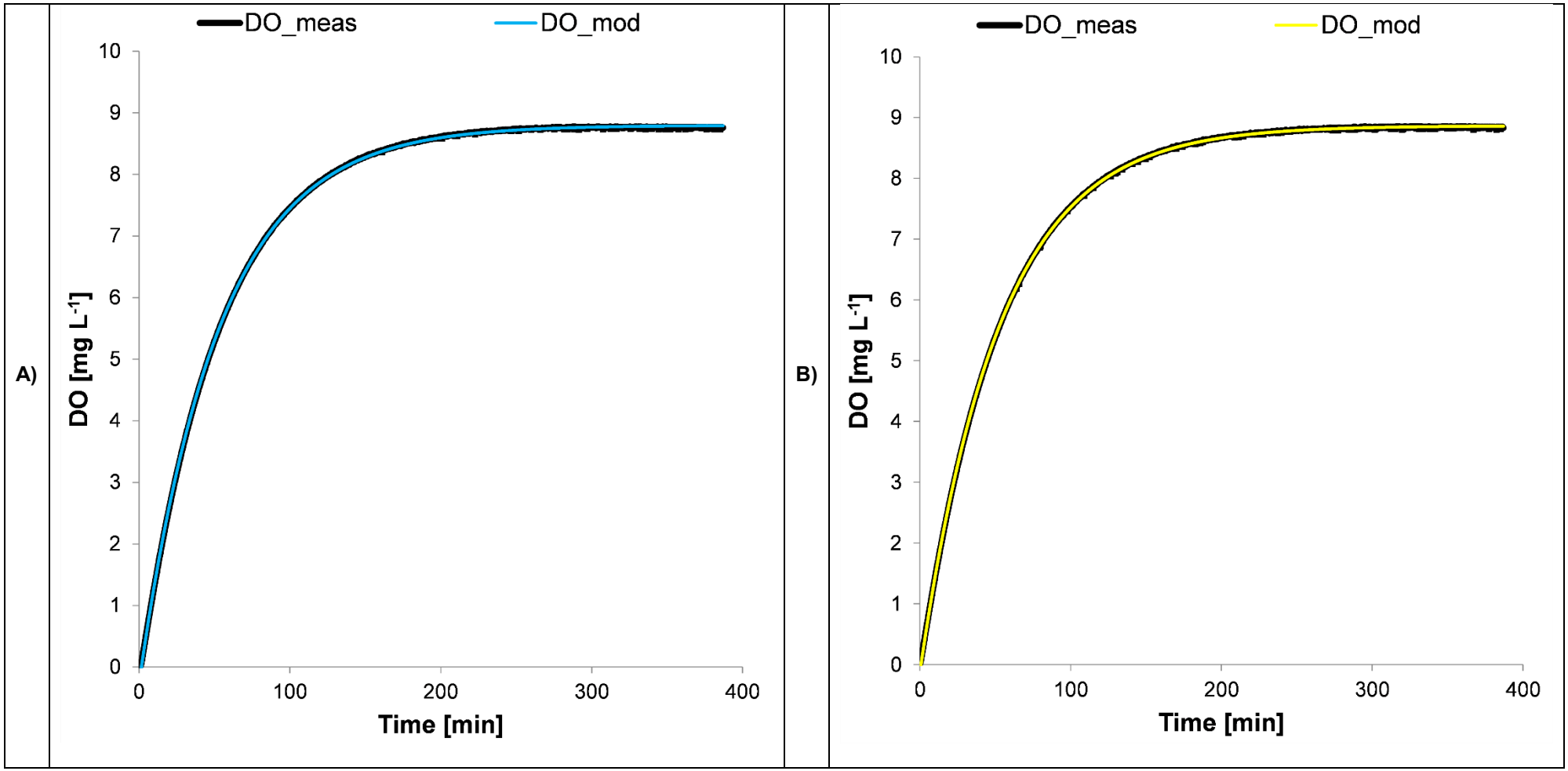

Figure SI.3. Re-aeration curves used for the evaluation of the volumetric mass transfer coefficient k_La in the control reactor (A) and in the inhibited reactor (B).

SI.6. SEPARATION EFFICIENCY FOR ALUMINIUM SULPHATE AND FERRIC CHLORIDE

The separation efficiency was calculated for the metal-based flocculants aluminium sulphate and ferric chloride, upon the exposure of MA samples at different metal concentrations and settling times. As shown in **Figure SI.4** and **Figure SI.5**, both flocculants allowed for a high removal efficiency (always higher than 94%), with small differences according to the operational conditions applied. However, it can be observed that, to achieve similar separation efficiencies, a higher dosage of iron is required, compared to aluminium. Indeed, with the same dosage of Al- and Fe-based flocculants, a higher separation efficiency is always obtained using aluminium sulphate. As an example, to achieve a comparably high separation efficiency (97-98%), a dosage of 100 mg Fe L^{-1} is required, compared to a dosage of 25 mg Al L^{-1}.

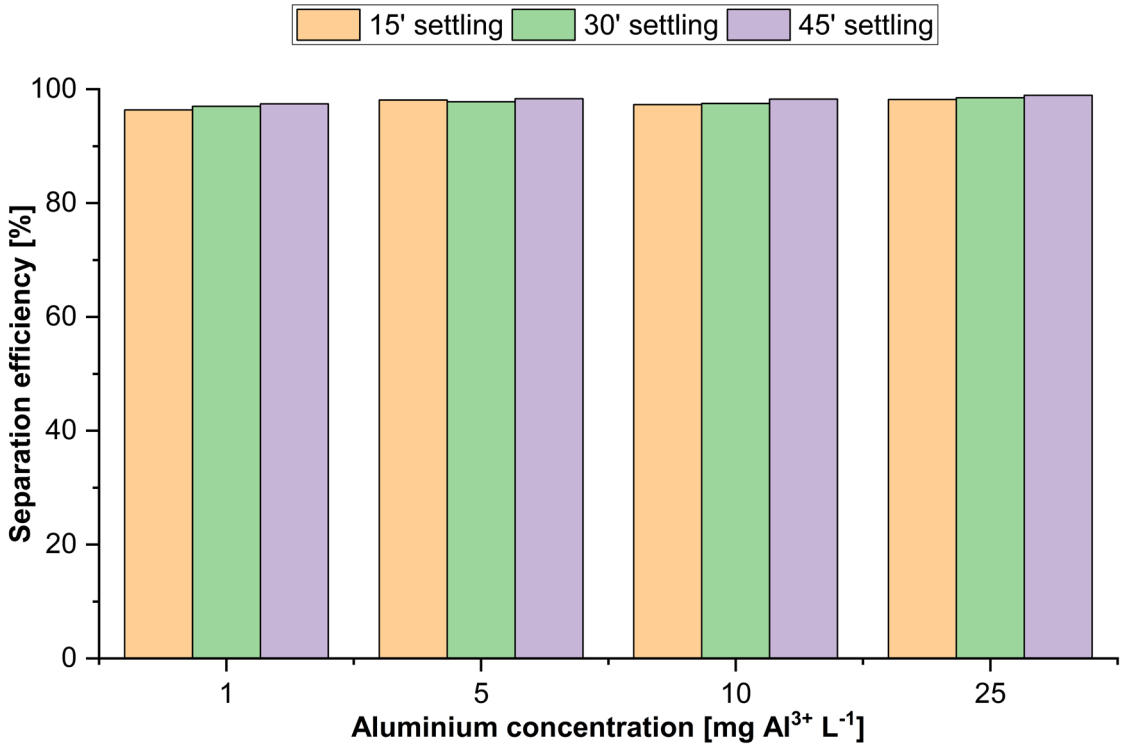

Figure SI.4. Separation efficiency of aluminium sulphate at different Al concentrations and settling times. The test was performed on MA samples.

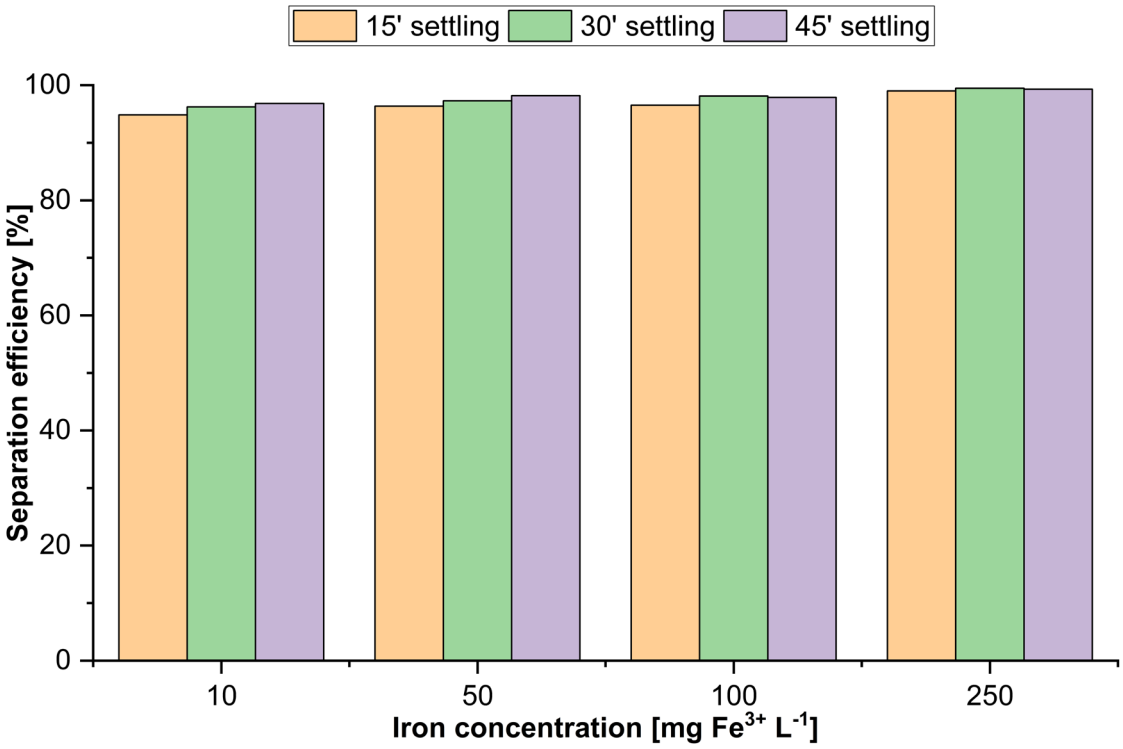

Figure SI.5. Separation efficiency of iron chloride at different Fe concentrations and settling times. The test was performed on MA samples.

SI.7. CALCULATION OF METALS PARTITIONING AMONG THE SOLID AND LIQUID PHASES

In order to evaluate the partitioning of metals among the solid and the liquid phases, dedicated experiments were conducted, as also detailed in **Section 2.5.1** of the manuscript. The calculation of metal fractions is given below:

$$\%SP = \frac{\text{Me mass (AP)}}{\text{Me mass (CF)}} * 100 \qquad \text{(Eq. SI .10)}$$

$$\%LP = \frac{\text{Me mass (SN)}}{\text{Me mass (CF)}} * 100 \qquad \text{(Eq. SI .11)}$$

Where: %SP is the percentage of the dosed metal ending up in the solid phase [%], %LP is the percentage of the dosed metal ending up in the liquid phase [%], Me mass (AP) is the mass of metal (Fe or Al) measured in the algal paste [g], Me mass (SN) is the mass of metal (Fe or Al) measured in the supernatant [g] and Me mass (CF) is the mass of metal (Fe or Al) measured in the algal suspension subject to coagulation-flocculation [g].

SI.8. IMPACTS OF LIGHT DISTRIBUTION AND SOLUTION COLOUR ON PHOTO-RESPIROMETRIC TESTS

Modelling of radiation transfer in the photo-respirometer

In the view of providing an estimation of the reduction of the average radiation intensity along the PBR optical thickness due to the increased absorbance of the liquid medium, a simple approach based on the Lambert-Beer law was applied, considering an exponential decay of light along the optical path from lamp external surface and reactor inner surface (4.5 cm). The estimation of the average radiation intensity along the optical path was performed as detailed in Christensen and Linden[7]:

$$\bar{I} = \sum_{\lambda} I_{0,\lambda} \frac{1-e^{-OD_{\lambda} \cdot L}}{OD_{\lambda} \cdot L} \qquad \text{(Eq. SI.12)}$$

Where: $\bar{I}$ is average radiation intensity along optical path L, $I_{0,\lambda}$ is the radiation intensity at lamp external surface at the specific wavelength λ and OD_{λ} is liquid medium absorbance at a specific wavelength λ. The emission spectrum of the light source (in μE m^{-2} s^{-1}) and the absorption spectrum of the liquid medium were considered with 10 nm step discretization. Other optical phenomena were neglected (light scattering, reflection and refraction by reactor walls, non-idealities of light source and reactor geometry).

The values of optical densities at the characteristic wavelengths of chlorophyll (420 nm and 680 nm) are given in **Table SI.4**. Complete light absorption spectra are reported in **Figure SI.6**.

Table SI.4. Evaluation of the ratio between the OD_{680} and OD_{420} at different concentrations of iron and aluminium flocculants. The control suspension was the same in both cases.

METAL [-]	CONCENTRATION [mg L^{-1}]	OD_{680} [-]	OD_{420} [-]	OD_{680}/OD_{420} [-]	Increase in the OD_{680} [%]	Increase in the OD_{420} [%]
None	0	0.19	0.23	0.81	0	0
Fe	10	0.22	0.31	0.81	14.3	34.8
Fe	50	0.23	0.40	0.82	23.3	72.5
Fe	100	0.26	0.54	0.80	39.7	133
Fe	250	0.24	0.59	0.74	24.9	151
Al	1	0.19	0.24	0.69	1.1	1.7
Al	5	0.20	0.25	0.58	6.3	5.6
Al	10	0.21	0.26	0.49	8.5	9.4
Al	25	0.20	0.26	0.40	3.2	12.9

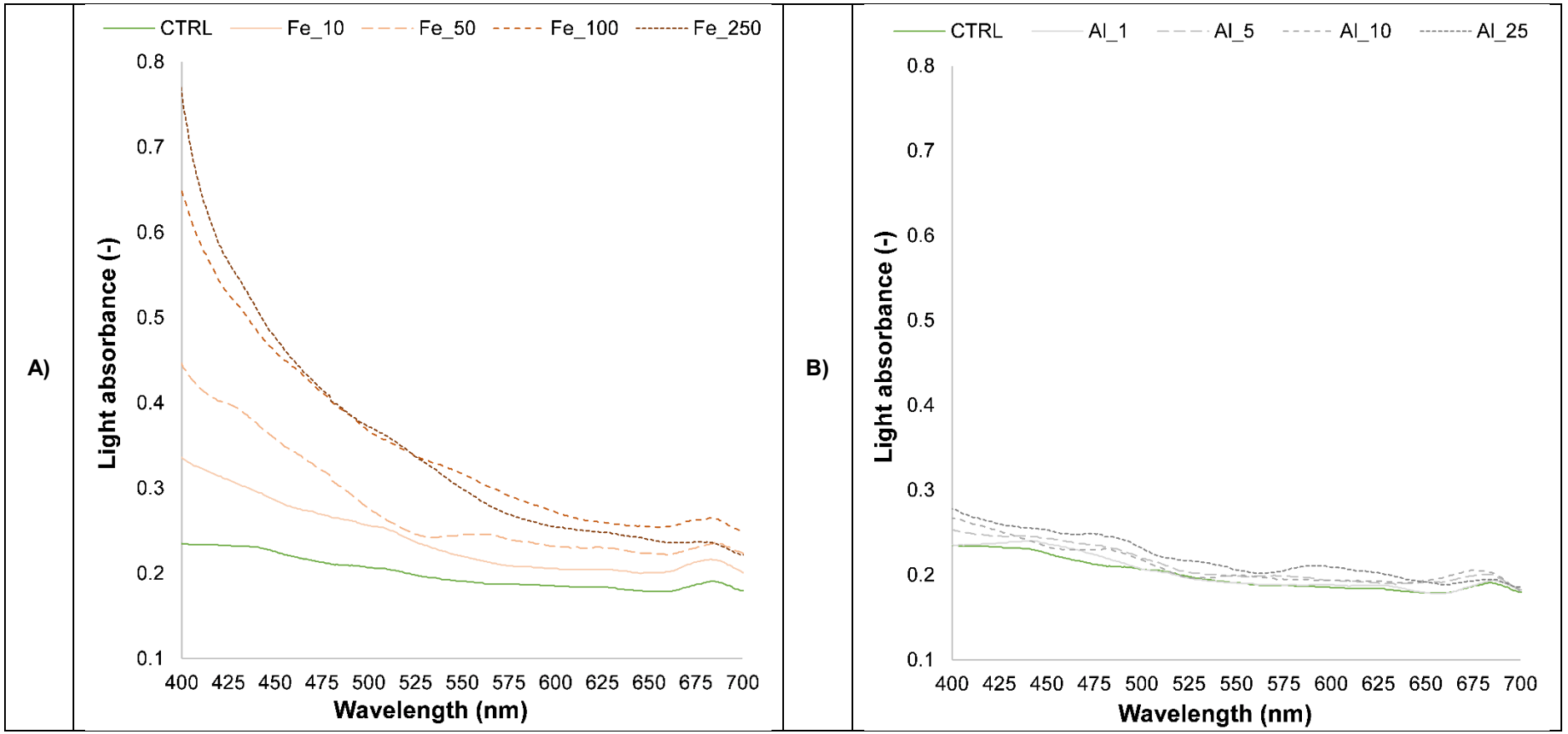

Figure SI.6. Light absorption in the microalgae suspension (MA), after the addition of concentrated solutions: (A) Fe (10, 50, 100 and 250 mg L^{-1}), (B) Al (1, 5, 10 and 25 mg L^{-1}). The control condition (no metals added, solid green line) was the same for both cases.

SI.9. RECOVERY OF PHOTOSYNTHESIS INHIBITION FROM METALS

To determine if the effect of photosynthesis inhibition from metallic flocculants persisted over time, the SCIP was performed after 1 h of exposure to Fe and Al, then the test was repeated after 24 h. The residual activities referred to the control condition with no metals added are reported in **Table SI.5**.

Table SI.5. Reversibility of inhibition from metallic flocculants in MA samples: residual activity evaluated 1 h and 24 h after the exposure to iron (100 mg Fe^{3+} L^{-1}) and aluminium (10 mg Al^{3+} L^{-1}).

METAL [-]	Residual activity after 1 h exposure [%]	Residual activity after 24 h exposure [%]
Fe	64.9 ± 0.9%	77.6 ± 1.1%
Al	67.3 ± 1.8%	94.6 ± 0.9%

SI.10. REFERENCES

(1) Marazzi, F.; Bellucci, M.; Rossi, S.; Fornaroli, R.; Ficara, E.; Mezzanotte, V. Outdoor Pilot Trial Integrating a Sidestream Microalgae Process for the Treatment of Centrate under Non Optimal Climate Conditions. *Algal Res.* **2019**, *39*, 101430. https://doi.org/10.1016/j.algal.2019.101430.

(2) Rossi, S.; Casagli, F.; Mantovani, M.; Mezzanotte, V.; Ficara, E. Selection of Photosynthesis and Respiration Models to Assess the Effect of Environmental Conditions on Mixed Microalgae Consortia Grown on Wastewater. *Bioresour. Technol.* **2020**, *305*, 122995. https://doi.org/10.1016/j.biortech.2020.122995.

(3) Rossi, S.; Díez-Montero, R.; Rueda, E.; Castillo Cascino, F.; Parati, K.; García, J.; Ficara, E. Free Ammonia Inhibition in Microalgae and Cyanobacteria Grown in Wastewaters: Photo-Respirometric Evaluation and Modelling. *Bioresour. Technol.* **2020**, *305*, 123046. https://doi.org/10.1016/j.biortech.2020.123046.

(4) Andreotti, V.; Solimeno, A.; Rossi, S.; Ficara, E.; Marazzi, F.; Mezzanotte, V.; García, J. Bioremediation of Aquaculture Wastewater with the Microalgae Tetraselmis Suecica: Semi-Continuous Experiments, Simulation and Photo-Respirometric Tests. *Sci. Total Environ.* **2020**, *738*, 139859. https://doi.org/10.1016/j.scitotenv.2020.139859.

(5) Sander, R. Compilation of Henry's Law Constants (Version 4.0) for Water as Solvent. *Atmospheric Chem. Phys.* **2015**, *15* (8), 4399–4981. https://doi.org/10.5194/acp-15-4399-2015.

(6) ASCE. Measurement of Oxygen Transfer in Clean Water. *ANSI/ASCE 2-91* **1993**.

(7) Christensen, J.; Linden, K. G. How Particles Affect UV Light in the UV Disinfection of Unfiltered Drinking Water. *J. AWWA* **2003**, *95* (4), 179–189. https://doi.org/10.1002/j.1551-8833.2003.tb10344.x.